Supporting Information

Oxophilicity Drives Oxygen Transfer at a Palladium-Silver Interface for Increased CO Oxidation Activity

Vikram Mehar[1,†], Abdulrahman Almithn[1,4,†], Tobias Egle[2,3], Ming-Hung Yu[1], Christopher R. O'Connor[2], Mustafa Karatok[2], Robert J. Madix[3], David Hibbitts[1] and Jason F. Weaver[1]*

[1]Department of Chemical Engineering, University of Florida, Gainesville, FL 32611, USA

[2]Department of Chemistry and Chemical Biology, Harvard University, Cambridge, MA 02138, USA

[3] School of Engineering and Applied Sciences, Harvard University, Cambridge, MA 02138, USA

[4]Department of Chemical Engineering, King Faisal University, Al-Ahsa, 31982, Saudi Arabia

[†] Vikram Mehar and Abdulrahman Almithn contributed equally to this work.

*To whom correspondence should be addressed, weaver@che.ufl.edu

Tel. 352-392-0869, Fax. 352-392-9513

S1. Sample mounting and cleaning

The Ag(111) crystal used in this study is a circular top-hat-shaped disk (10 mm × 1.65 mm) cut to isolate the (111) surface plane within a tolerance of ± 0.1°. The Ag(111) crystal was mounted on W wires and attached to a copper sample holder that is in thermal contact with a liquid nitrogen cooled reservoir. A type K thermocouple was attached to a small hole on the side of the crystal. The sample is resistively heated and the temperature is controlled using a PID controller that adjusts the output of a dc power supply. In this setup, we are able to maintain or linearly ramp the sample temperature from 89 to 800 K. Sample cleaning consisted of cycles of sputtering with 2000 eV Ar^+ ions at a surface temperature of 300 K, followed by annealing at 800 K for 5 min in UHV. The Ag(111) sample was considered to be clean when Auger electron spectra exhibited no discernable signals for the C(KLL), S(KLL) and O(KLL) peaks and a sharp LEED pattern characteristic of Ag(111) was observed.

S2. O_2 TPD spectrum from single-layer AgO_x/Ag(111)

Figure S1 shows the thermal desorption spectrum obtained from an ~0.38 ML single-layer AgO_x on Ag(111). The O-atom beam was exposed to pristine Ag(111) at 515 K and the sample was heated to 535 K in UHV. The spectrum exhibits a single sharp peak at 570 K arising from the decomposition of dominant p(4 x 5√3) phase where small amount of p(4 x 4) and c(3 x 5√3) phases also exist. The spectrum obtained is in good agreement with prior TPD characterization of the pure single-layer AgO_x structures.[1-3] We note that post heating to 535 K in UHV causes negligible decomposition of the 0.4 ML single-layer AgO_x phase.

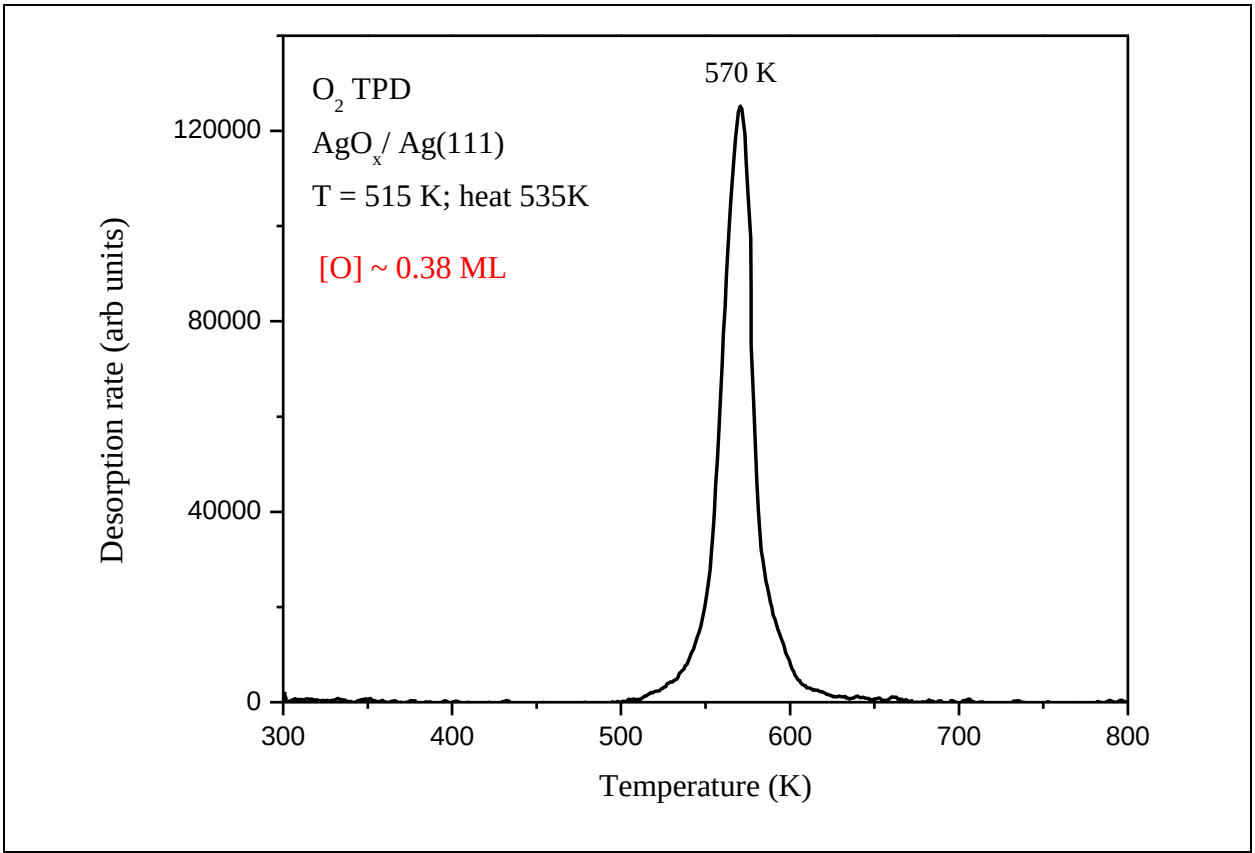

Figure S1. O_2 TPD obtained after 2 min of atomic oxygen exposure with the sample held at 515 K followed by heating to 535 K in UHV.

S3. Structural models of single-layer AgO_x/Ag(111) phases

Figure S2 displays the structural models for the three known phases of single-layer AgO_x. The p(4 x 4) model (Fig. S2a) consists of 12 Ag atoms present in two Ag_6 triangles with each Ag atom sitting on top of threefold sites of the underlying Ag(111) substrate. These triangular units are separated by two oxygen atoms located in the trough and the unit cell consists of a total of 6 O atoms resulting in a stoichiometry of Ag_2O. The rectangular unit cells of c(3 x 5√3) and p(4 x 5√3) phase (Fig. S2b and c) are composed of clusters of Ag hexamers and decamers separated by a row of oxygen atoms located in the furrows.

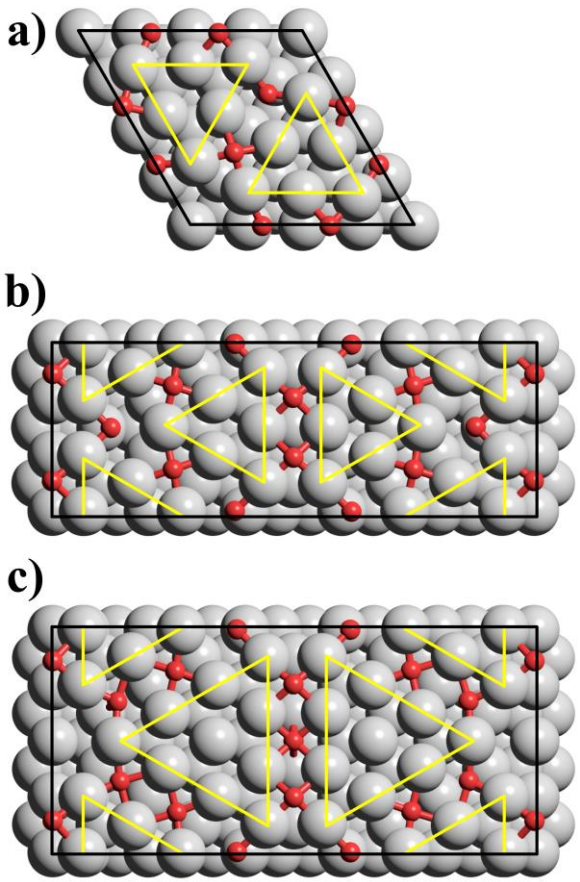

Figure S2. Optimized structures for the three AgO_x phases: (a) p(4 × 4), (b) c(3 × 5√3), and (c) p(4 × 5√3) on 4-layer Ag(111) slabs. Triangular-shaped Ag_6 and Ag_{10} units are highlighted in yellow and the unit cells are indicated by black lines. Color code: O (red), Ag (gray).

S4. Relationships between edge and terrace sites of bi-layer Pd clusters

We developed mathematical relationships to calculate the number of Pd atoms located at the surface and edges of hexagonal Pd bi-layer clusters of varying size. These relationships were developed for hexagonal clusters with the same shape as the Pd_{46} cluster used in our DFT calculations. As seen in Figure 1c, the top layer of the Pd_{46} cluster is comprised of close-packed Pd atoms arranged into a regular hexagon with sides of $2a$ in length, where a = 0.277 nm is the Pd(111) lattice constant. The bottom layer is also a hexagonal, close-packed arrangement with alternating sides of length $2a$ and $3a$. In our geometric model, we consider clusters in which the top layer is hexagonal with sides of na in length and the bottom layer is hexagonal with alternating sides of na and $(n + 1)a$ in length where n is an integer. The maximum diameter of a bi-layer cluster is specified as the distance between opposing corners of the bottom hexagonal layer and is given by the expression: $D_{max} = (2n + 1)a$.

Relationships between the number of different types of Pd atoms and the cluster size were developed for the bottom and top layers by determining how the number of triangular arrangements of atoms in each layer vary with n and weighting the atoms located in the interior, edges and corners by factors of $\frac{1}{6}$, $\frac{1}{3}$ and $\frac{1}{2}$, respectively, where these values represent the reciprocal of the number of triangular arrangements that share each type of atom. We find the following relationships:

Top layer, Number of corner + edge atoms: $N_E^{top} = 6 + 6(n - 1)$

Top layer, Number of interior atoms: $N_I^{top} = 3n^2 - 3n + 1$

Bottom layer, Number of corner + edge atoms: $N_E^{bottom} = 6 + 3(2n - 1)$

Bottom layer, Number of interior atoms: $N_I^{bottom} = 3n^2$

Total number of Pd atoms: $N_{tot} = N_E^{bottom} + N_I^{bottom} + N_E^{top} + N_I^{top}$

Number of surface Pd atoms: $N_{surf} = N_E^{bottom} + N_E^{top} + N_I^{top}$

Number of edge Pd atoms: $N_E = N_E^{bottom} + N_E^{top}$

Table S1. Structural characteristics of model hexagonal Pd bi-layer clusters of varying size. The shapes of the clusters are described in the text and are characterized by the integer *n*, where the top layer of the cluster is a regular hexagon with sides of length *na* where *a* is the lattice constant of Pd(111). The table lists the maximum diameter (nm), the total number of Pd atoms, the percentage of surface Pd atoms at edges and the number of surface Pd atoms for clusters as a function of *n*. Also listed are the equivalent number of Ag(111) atoms of the bottom layer of each cluster and the area-scaled number of surface Pd atoms, as described in Section S4.

n	D_{max} (nm)	Total number of Pd atoms	Percentage of surface Pd atoms at edges (N_E/N_{surf})*100	Number of surface Pd atoms	Equivalent number of Ag(111) atoms of bottom layer	Area-scaled number of surface Pd atoms (surface atoms/ ML-surfPd)
1	0.83	19	94%	16	5.9	2.70
2	1.39	46	79%	34	16.9	2.01
3	1.94	85	67%	58	33.3	1.74
4	2.49	136	58%	88	55.2	1.59
5	3.05	199	51%	124	82.6	1.50
6	3.60	274	45%	166	115.4	1.44
7	4.16	361	41%	214	153.7	1.39
8	4.71	460	37%	268	197.5	1.36
9	5.26	571	34%	328	246.8	1.33
10	5.82	694	31%	394	301.5	1.31
11	6.37	829	29%	466	361.7	1.29
12	6.93	976	27%	544	427.4	1.27

Table S1 lists the total number of Pd atoms, the number of surface Pd atoms and the percentage of surface Pd atoms at edges for *n* = 1 to 12 as well as the maximum diameters. The percentage of edge Pd atoms decreases from 94% to 27% as the maximum diameter increases from roughly 1 to 7 nm, scaling nearly as 1/*n*. Table S1 also shows the equivalent number of Ag(111) atoms in the bottom layer of each cluster, which was determined by dividing the area of the bottom layer by the area of the primitive unit cell of Ag(111) (A(Ag(111)) = 0.073 nm^2) and setting the number of

atoms in each Ag(111) unit cell to one. The area-scaled number of surface Pd atoms is then defined as the number of surface Pd atoms divided by the equivalent number of Ag(111) atoms of the bottom layer; this quantity is expressed in units of number of surface Pd atoms per ML-surfPd. As reported in the main manuscript, this area-scaled number of surface atoms may be used to convert coverages referenced to the Pd-Ag(111) contact area (ML/ML-surfPd) to a ratio of adsorbates per surface Pd atom, thus providing a more accurate estimate of the local density of adsorbates on small Pd clusters.

Table S2 shows the amount of oxygen removed by CO oxidation and the initial CO coverage as a function of the total Pd coverage, as estimated from TPRS data collected after saturating the surfaces with CO at 100 K. Based on a comparison with XPS data collected prior to CO adsorption, the amount of oxygen removed is concluded to be approximately equal to the initial oxygen coverage on the Pd. The oxygen and CO coverages are listed in units of ML per ML-surfPd, which were obtained by dividing the total amount of O and the initial CO coverage determined from TPRS by the surface Pd coverage estimated previously.[4] We converted these coverages into ratios of the number of O or CO adsorbates per Pd surface atom by scaling with estimates of the number of surface Pd atoms per ML-surfPd as given in Table S1 for clusters of the appropriate size. Analysis of previously-reported STM images estimates an average cluster diameter of ~3 nm for Pd coverages of 0.30 and 0.45 ML and ~6 nm for a Pd coverage of 0.90 ML; we neglect edge sites in this analysis for the nearly conformal bi-layer film that forms at [Pd] = 1.8 ML. From Table S1, cluster diameters of ~3 and 6 nm correspond approximately to the n = 5 and 10 clusters for which our geometric model predicts that the area-scaled numbers of surface Pd atoms are 1.5 and 1.3 per ML-surfPd, respectively. Scaling by these factors gives estimates of the O and CO coverages per Pd_{surf} atom as shown in Table S2.

Table S2. Amount of oxygen removed by CO and initial CO coverage as a function of the total Pd coverage generated on the AgO_x single layer. Estimates of the surface Pd coverages (ML-surfPd) are also given as described in main manuscript. The ratios $O:Pd_{surf}$ and $CO:Pd_{surf}$ were computed using predictions of the geometric model for Pd bi-layer clusters with sizes given by n = 5 ([Pd] = 0.30 and 0.45 ML) and n = 10 ([Pd] = 0.90 ML), which were selected based on estimates of the average cluster diameters (~3 and 6 nm) at these coverages determined from previously reported STM images.[4] Contributions from edge sites were neglected for the 1.8 ML Pd bi-layer. The estimated Pd_{edge} site fractions are also shown.

[Pd] (ML)	[Pd] (ML-surfPd)	[Pd_{edge}] (Pd_{edge}:Pd_{surf})	[O] (ML O/ML-surfPd)	[O] ($O:Pd_{surf}$)	[CO] (ML O/ML-surfPd)	[CO] ($CO:Pd_{surf}$)
0.30	0.18	0.50	0.74	0.49	1.03	0.69
0.45	0.21	0.50	0.81	0.54	1.18	0.79
0.90	0.49	0.30	0.43	0.33	0.66	0.51
1.8	0.95	~0	0.39	0.39	0.59	0.59

S5. Analysis of O 1s and Pd 3d spectra acquired from Pd deposited on AgO_x/Ag(111)

We have recently reported Pd 3d and O 1s spectra obtained after depositing varying amounts of Pd onto the AgO_x single layer at 300 K.[4] Details of the apparatus and conditions used in acquiring the X-ray photoelectron spectra are described previously.[4-5] All spectra were obtained using Mg Kα X-rays (hν = 1253.6 eV) generated from a laboratory X-ray source. Deconvolution of the Pd $3d_{5/2}$ spectra provides estimates of the fraction of partially oxidized Pd as a function of the Pd coverage from ~0.15 to 2.5 ML as shown previously.[4] Table S1 summarizes these fractions and Figure S3 shows a representative Pd 3d spectrum acquired after depositing ~2.5 ML of Pd onto the AgO_x surface. This Pd $3d_{5/2}$ spectrum can be accurately fit by constraining the total percentage of oxidized Pd to ~16%, which is assumed to represent the fraction of oxidized Pd that results when all of the oxygen from the AgO_x transfers to 2.5 ML of Pd.

In the present study, we computed difference O 1s spectra to estimate the amount of oxygen transferred from AgO_x to Pd after deposition at 300 K as a function of the Pd coverage. The difference O 1s spectra were obtained by subtracting the O 1s spectrum obtained from the clean AgO_x/Ag(111) surface from those collected after depositing Pd onto the AgO_x layer. The O 1s spectrum obtained from the pure AgO_x layer exhibits a single peak at 528.4 eV (Figure S4a). This

peak diminishes after Pd deposition due to oxygen transfer from AgO_x to Pd (Figure S4b); a new O 1s peak associated with O bonded to Pd is masked by the main Pd 3p peak that appears in the O 1s spectral region near 532 eV.[6] Difference O 1s spectra are shown in Figures S4c-h for different Pd coverages. The loss of O 1s area near 528.4 eV is assumed to be proportional to the amount of oxygen that transferred from AgO_x to Pd and indeed increases with increasing Pd coverage. The amount of oxygen transferred is computed in units of ML by scaling the "negative" area in the difference O 1s spectrum by the area of the O 1s spectrum obtained from the pure AgO_x layer and assuming that the pure AgO_x surface has an O coverage of 0.38 ML. Notably, inelastic scattering of photoelectrons moving through Pd would cause the O 1s peak from the AgO_x layer to diminish with increasing Pd coverage, even if oxygen transfer was negligible. Given that Pd domains cover a fraction *f* of the AgO_x layer, where *f* has been determined from STM measurements, the following equation may be used to estimate the attenuation of the AgO_x O 1s signal that could be caused by the deposited Pd,

$$I/I_o = (1 - f) + f*\exp(-D_{Pd}/\lambda)$$

where I and I_o are the intensities of the O 1s peak at 528.4 eV for Pd-decorated and pure AgO_x layers, respectively, D_{Pd} = 4.4 Å is the approximate thickness of a Pd(111) bi-layer and λ = 13.3 Å is the inelastic mean free path of electrons with 723 eV kinetic energy traveling through Pd. Using this equation, we estimate that inelastic scattering could account for only about 20% of the decrease in the O 1s peak intensity from the AgO_x phase observed after Pd deposition for the Pd coverages studied. This comparison supports the conclusion that the observed decrease in the O 1s peak from AgO_x is caused by oxygen transfer from AgO_x to Pd. A summary of the amount of oxygen transferred as a function the Pd coverage is given in Table S3. The fraction of oxidized Pd and the amount of oxygen transferred, determined from the Pd 3d and difference O 1s spectra,

respectively, agree well thus suggesting that the fraction of oxidized Pd is also representative of the amount of oxygen transferred to the Pd.

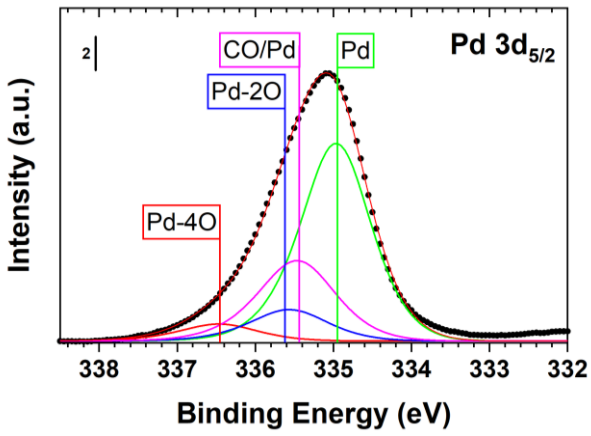

Figure S3. Pd $3d_{5/2}$ spectrum obtained from 2.5 ML Pd deposited on AgO_x/Ag(111) at 300 K.

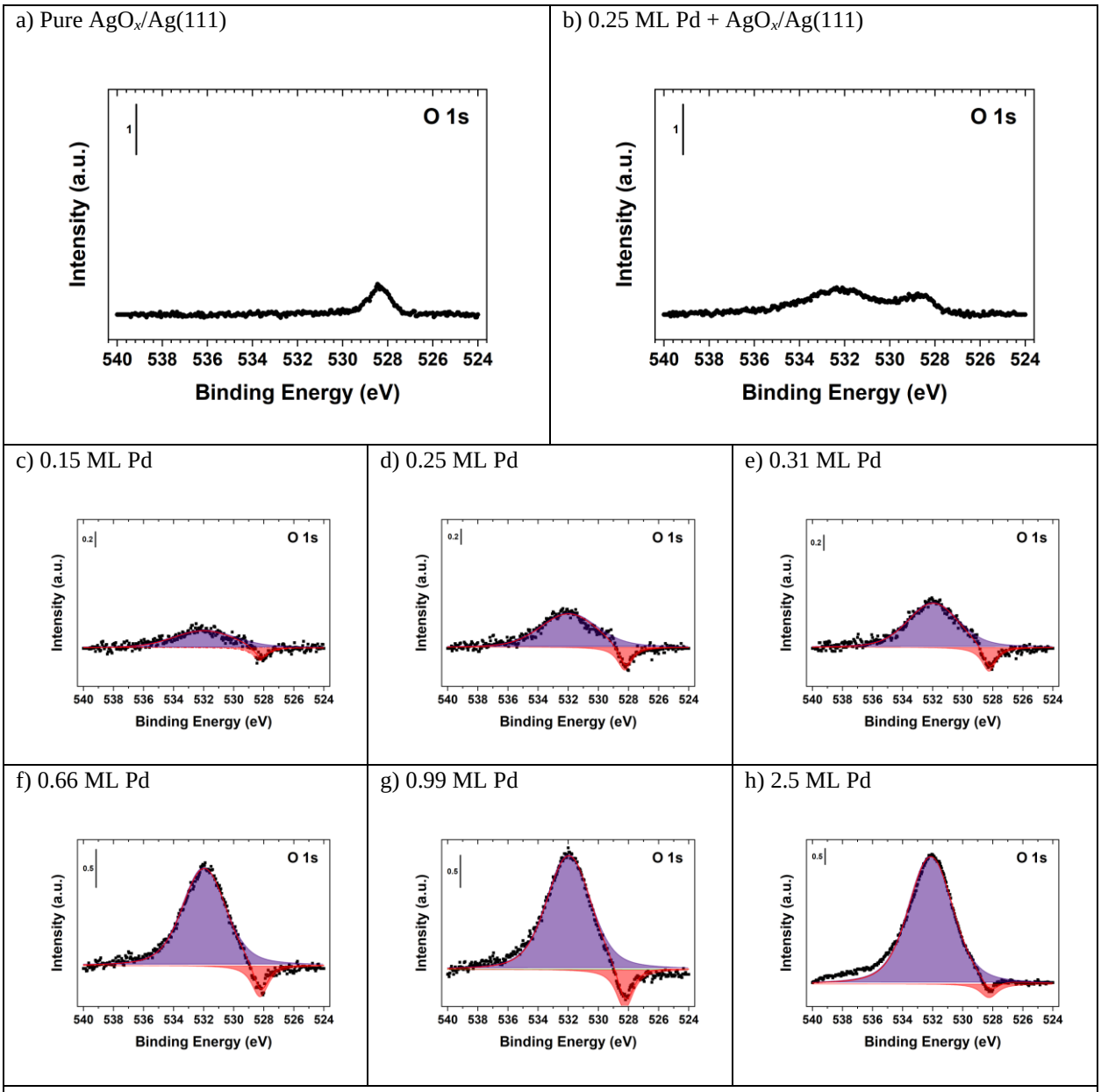

Figure S4. O 1s spectra obtained from a) the pure AgO$_x$/Ag(111) and b) 0.25 ML Pd deposited on the AgO$_x$ layer. c-h) Difference O 1s spectra for varying coverages of Pd prepared by deposition onto the single-layer AgO$_x$/Ag(111) surface at 300 K. Each spectrum was obtained by subtracting the O 1s spectrum acquired from the pure AgO$_x$ single-layer from that acquired after depositing a specific amount of Pd. A decrease in the amount of AgO$_x$ on the surface due to oxygen transfer from AgO$_x$ to Pd is assumed to be responsible for the loss of area near 528.4 eV in the O 1s difference spectrum (red). Photoemission from the Pd 3p core-level makes the dominant contribution to the intense peak near 532 eV (purple). The amount of oxygen transferred is computed in units of ML by scaling the "negative" area in the difference O 1s spectrum by the area of the O 1s spectrum obtained from the pure AgO$_x$ layer and assuming that the pure AgO$_x$ surface has an O coverage of 0.38 ML.

Table S3. Fraction of oxidized Pd, total O transferred from AgO_x to Pd and the oxygen coverage on Pd as a function of the total Pd coverage generate on AgO_x at 300 K. The fraction of oxidized Pd is equal to the fraction of the total Pd $3d_{5/2}$ area that was fit with components for Pd-2O + Pd-4O species.[4] The total O transferred was determined from O 1s difference spectra as described in the text. Also shown are the surface Pd coverages and the oxygen coverage on Pd, the latter given in units of ML O/ML-surfPd. The surface Pd coverages were determined using a linear correlation between the total Pd coverage and fraction of the AgO_x surface covered by Pd that was reported recently from STM measurements.[4] The oxygen coverage on Pd is computed by averaging the fraction of oxidized Pd and the total O transferred and dividing by the surface Pd coverage.

Total Pd coverage (ML)	Fraction of oxidized Pd	Total O transferred (ML)	Surface Pd coverage (ML-surfPd)	Oxygen coverage on Pd (ML O/ML-surfPd)
0.15	0.06	0.06	0.19	0.31
0.25	0.10	0.11	0.13	0.78
0.31	0.13	0.12	0.18	0.71
0.66	0.21	0.17	0.35	0.55
0.99	0.24	0.26	0.52	0.47
2.5	0.39	0.41	1	0.39

S6. DFT-computed energies of oxygen transfer to a Pd single-layer

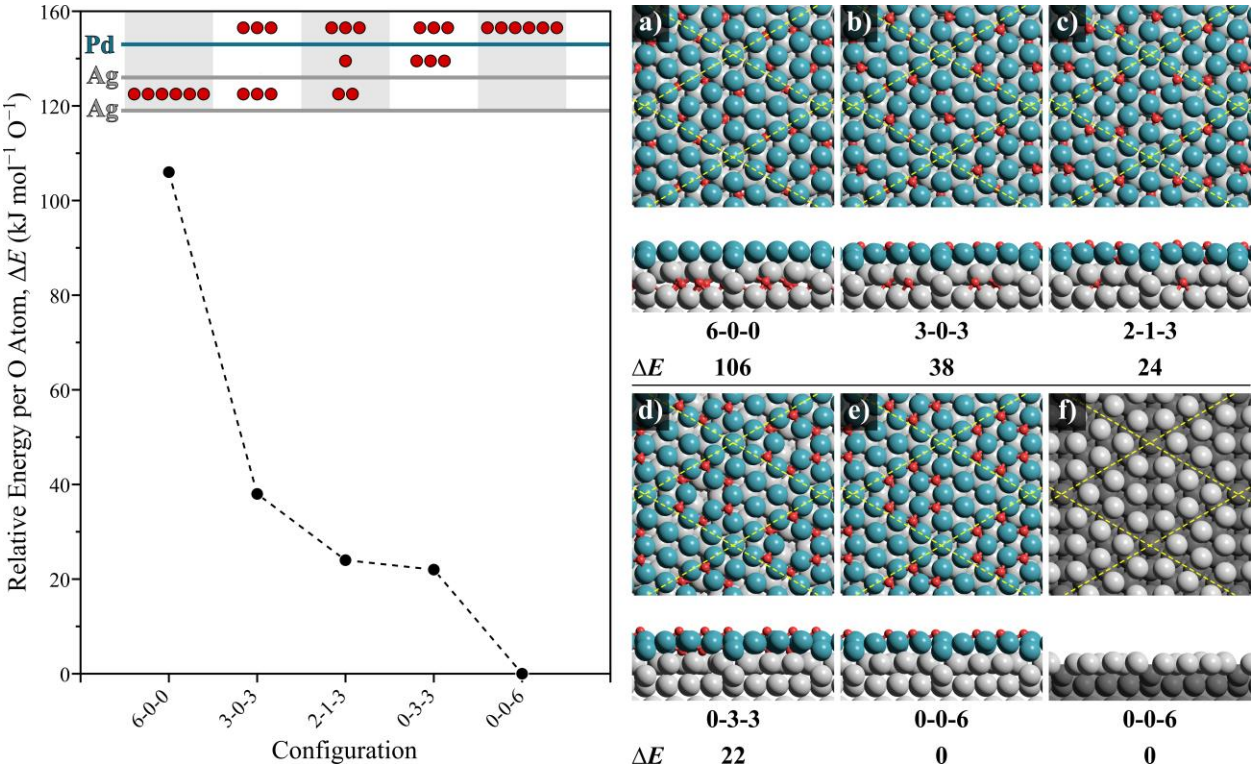

Figure S5. (*Left*) DFT-predicted relative energies, normalized per O-atom, for O configurations in the 4 × 4 single Pd overlayer on the AgO_x surface. (*Right*) Optimized structures shown for each O configuration (a-e). The image in (f) shows the arrangement of Ag atoms beneath the Pd single layer after all oxygen atoms moved to the Pd layer as shown in (e). Color code: O (red), Ag (gray), Pd (dark Cyan).

S7. DFT computed energies of O configurations on the Pd bi-layer

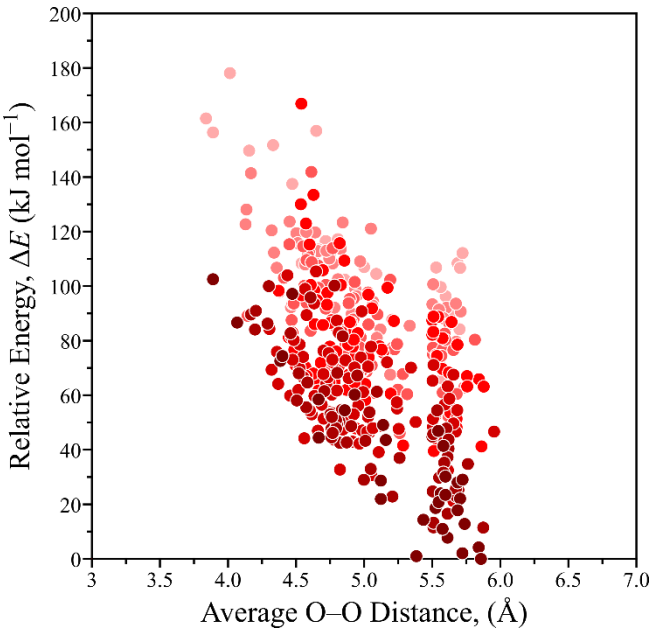

Figure S6. Energies for the examined 434 unique configurations of the 0-0-0-6 arrangement (where all 6 O atoms are above the Pd surface) relative to the most stable configuration as a function of average O–O distance in Å on the 4 × 4 bi-layer Pd overlayer model. The color gradient represents the number of O bound to the 3-fold fcc sites where darker red indicates more O on fcc sites rather than hcp sites.

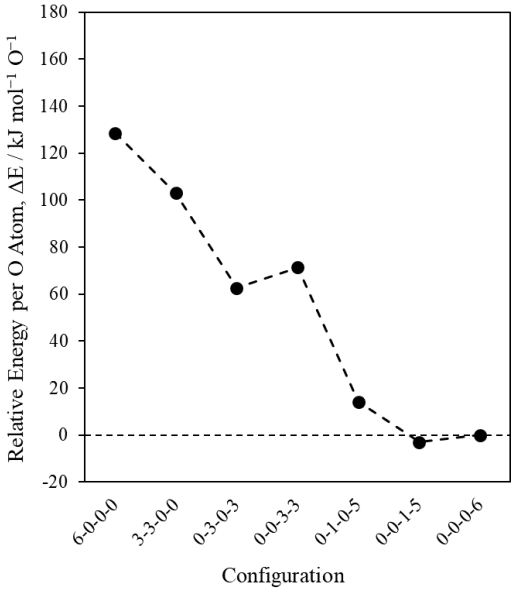

Figure S7. DFT-predicted relative energies, normalized per O-atom, for O configurations on the 4 × 4 bi-layer Pd overlayer on the AgO_x surface.

S8. Additional O configurations on the Pd_{46} cluster on AgO_x

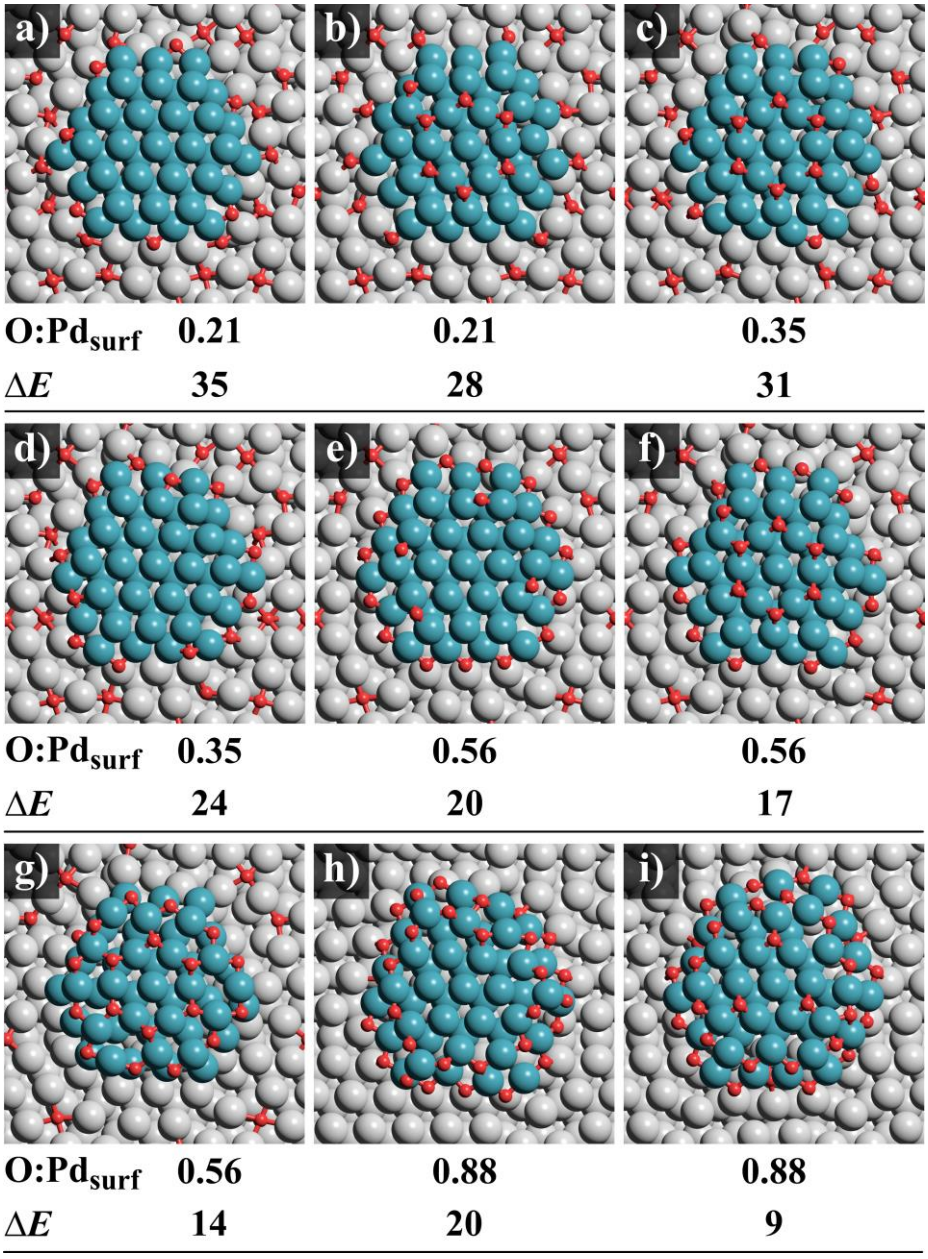

Figure S8. Other examined configurations for oxygen atoms on the bi-layer Pd_{46} hemispherical particle model not shown in Figure 5. Shown beneath image are oxygen coverage per total Pd atoms and the energies relative to the most stable configuration (Fig. 5e) normalized by the number of oxygen atoms (30 atoms). Color code: O (red), Ag (gray), Pd (dark Cyan).

S9. C-O stretch frequencies of CO on the Pd bi-layer on AgO_x: Influence of adsorbed O

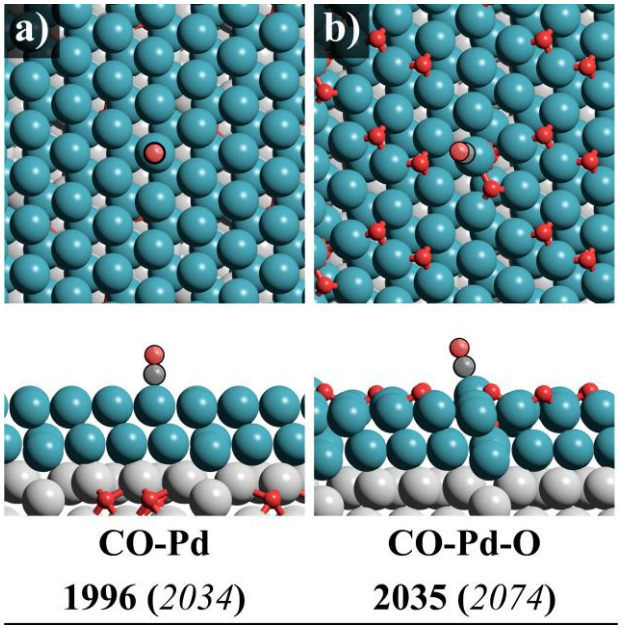

Figure S9. DFT-predicted C–O stretch frequencies for the (a) CO-Pd and (b) CO-Pd-O species on the 4 × 4 bi-layer Pd overlayer model in cm^{-1}. Shown in parentheses are the corrected frequencies using a scaling factor of 1.019 chosen to match gas-phase CO frequencies. Color code: O (red), Ag (gray), Pd (dark Cyan), C (dark gray).

S10. CO RAIRS as a function of Pd coverage on AgO_x

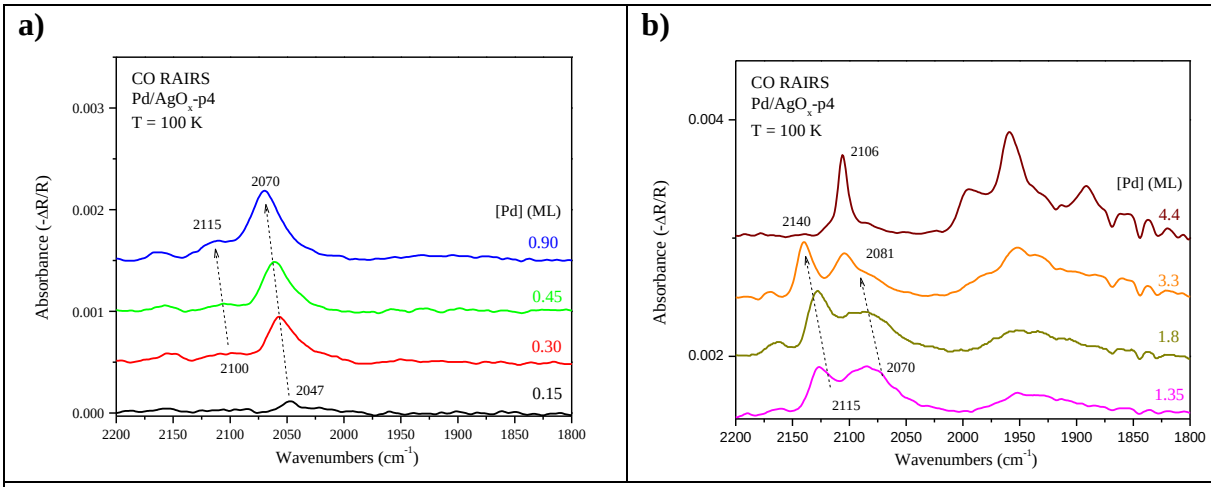

Figure S10. CO RAIRS obtained from Pd-AgO_x/Ag(111) surfaces after saturating with CO at 100 K for Pd coverages of a) [Pd] = 0.15, 0.30, 0.45 and 0.90 ML and b) [Pd] = 1.35, 1.8, 3.3 and 4.4 ML.

S11. TPRS after adsorbing CO on Pd-AgO_x/Ag(111): Variation with Pd coverage

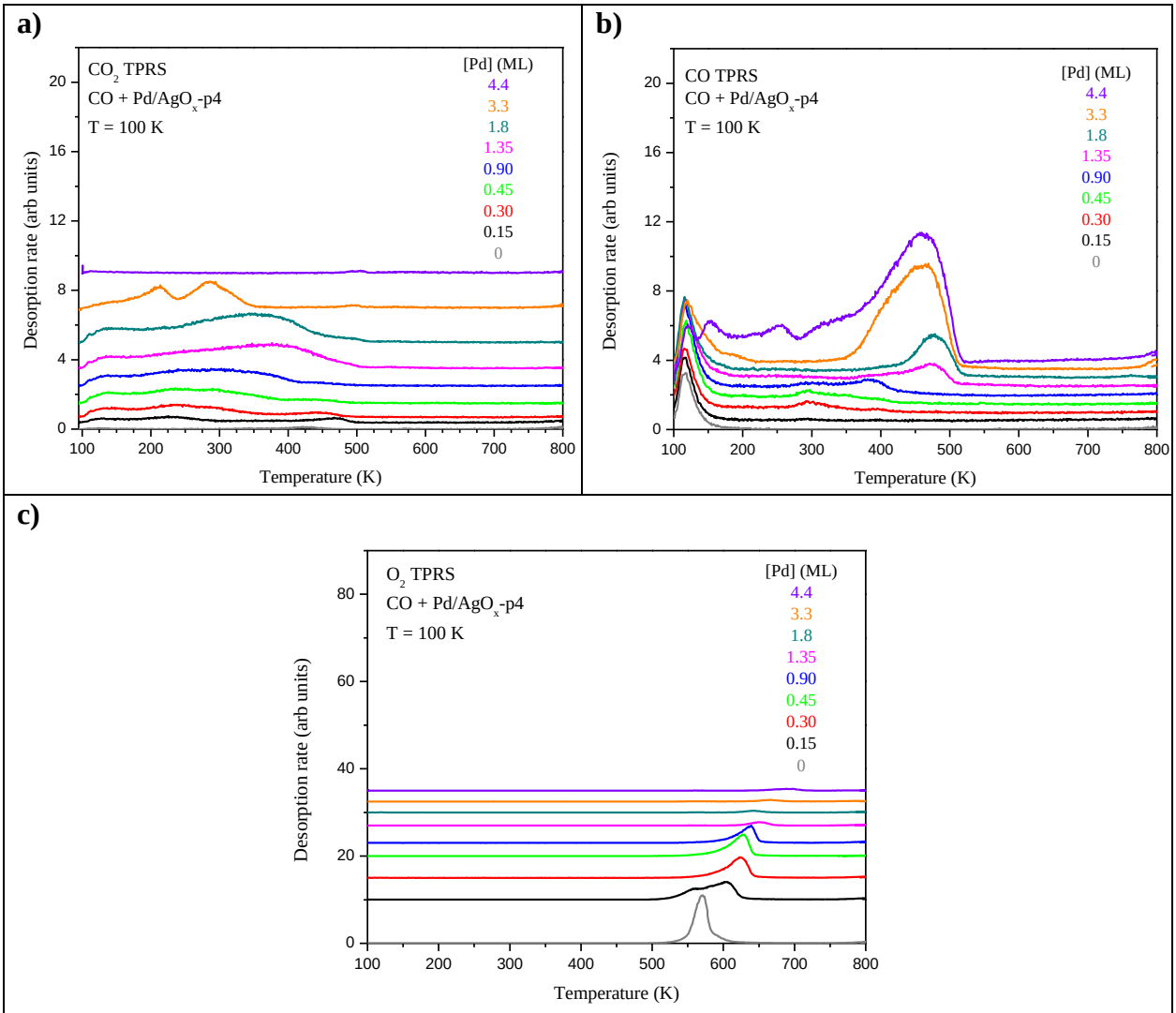

Figure S11. TPRS series for a) CO_2, b) CO and c) O_2 obtained as a function of the Pd coverage deposited onto single-layer AgO_x/Ag(111) after saturating each surface with CO at 100 K. Data are shown for Pd coverages from 0 to 4.4 ML, where the highest Pd coverage produces two layers of bi-layer Pd film that nearly completely covers the surface.

References

1. Derouin, J.; Farber, R. G.; Heslop, S. L.; Killelea, D. R., Formation of surface oxides and Ag2O thin films with atomic oxygen on Ag(111). *Surf. Sci.* **2015**, *641*, L1-L4.
2. Derouin, J.; Farber, R. G.; Turano, M. E.; Iski, E. V.; Killelea, D. R., Thermally Selective Formation of Subsurface Oxygen in Ag(111) and Consequent Surface Structure. *ACS Catal* **2016**, *6*, 4640-4646.
3. Campbell, C. T., Atomic and Molecular-Oxygen Adsorption on Ag(111). *Surf. Sci.* **1985**, *157*, 43-60.
4. Mehar, V.; O'Connor, C. R.; Egle, T.; Karatok, M.; Madix, R. J.; Friend, C. M.; Weaver, J. F., Growth and auto-oxidation of Pd on single-layer AgO_x/Ag(111). *Phys. Chem. Chem. Phys.* **2020**, *22*, 6202-6209.
5. van Spronsen, M. A.; Daunmu, K.; O'Connor, C. R.; Egle, T.; Kersell, H.; Oliver-Meseguer, J.; Salmeron, M. B.; Madix, R. J.; Sautet, P.; Friend, C. M., Dynamics of Surface Alloys: Rearrangement of Pd/Ag(111) Induced by CO and O-2. *J. Phys. Chem. C* **2019**, *123*, 8312-8323.
6. Lundgren, E.; Kresse, G.; Klein, C.; Borg, M.; Andersen, J. N.; De Santis, M.; Gauthier, Y.; Konvicka, C.; Schmid, M.; Varga, P., Two-dimensional oxide on Pd(111). *Phys. Rev. Lett.* **2002**, *88*, 246103.